Modelling the effects of short and random proto-neural elongations
Supplementary Material

Oltman O. de Wiljes[a,b], R.A.J. van Elburg[c], and Fred A. Keijzer[a,b]

[a]Theoretical Philosophy, University of Groningen
[b]Research School of Behavioural and Cognitive Neurosciences, University of Groningen
[c]Institute of Artificial Intelligence, University of Groningen

Supplementary Material 1: Distant connection implementation details

Regarding implementation details, consider the case of cells arranged in a plane. Every elongated cell extends an axodendritic elongation p with length l_p in an arbitrary direction ϕ_p, relative to the x-axis. Where elongations cross each other they create bidirectional connections between the originating cells. Given any two cells i and j with coordinates (x_i, y_i) and (x_j, y_j) and elongation directions relative to the x-axis ϕ_i and ϕ_j respectively, a triangle emerges, with at one point cell i, another point cell j and the third point the crossing of their elongations. Two sides of this triangle consist of the elongations themselves. The third side, d, is the line between the cells, with an angle relative to the x-axis: ϕ_d. Assuming $\phi_i \neq \phi_j \neq \phi_d$[1], the sine-rule allows us to locate the crossing location, given the angles and the locations of the cells.

$$\frac{d}{\sin(\phi_j - \phi_i)} = \frac{\rho_i}{\sin(\pi - \phi_j + \phi_d)} = \frac{\rho_j}{\sin(\phi_i - \phi_d)} \tag{1}$$

[1]In practice, given the granularity of the random numbers used, this assumption always holds.

Furthermore,

$$\sin(\pi - \phi_j + \phi_d) = -\sin(-\phi_j + \phi_d) = \sin(\phi_j - \phi_d) \tag{2}$$

Cell coordinates allow us to calculate d and ϕ_d:

$$d = \sqrt{(x_i - x_j)^2 + (y_i - y_j)^2} \tag{3}$$

$$\phi_d = \arctan\left(\frac{y_j - y_i}{x_j - x_i}\right) \tag{4}$$

Then we can solve for ρ_i and ρ_j:

$$\rho_i = d \cdot \frac{\sin(\phi_j - \phi_d)}{\sin(\phi_j - \phi_i)} \tag{5}$$

$$\rho_j = d \cdot \frac{\sin(\phi_i - \phi_d)}{\sin(\phi_j - \phi_i)} \tag{6}$$

If, for a given pair of cells, ρ_i and ρ_j are shorter than l_p, so $0 < \rho_i < l_p$ and $0 < \rho_j < l_p$, the cells are connected. We loosened this constraint to $-\frac{1}{2} < \rho_i < l_p$ and $-\frac{1}{2} < \rho_j < l_p$ to account for crossings occurring on the cell body of the originating cell.

All the above, however, is predicated on an infinite plane, while our system is finite and tube-shaped. Although a tube is essentially a curved 2-dimensional plane, its contiguousness results in some particular cases: elongations which may wrap around the cylinder. If we assume the cylinder is formed by making the x-direction periodic, we should consider not only the crossing of elongations starting at (x_i, y_i) and (x_j, y_j) but also at $(x_i + k_i \cdot \odot, y_i)$ and $(x_j + k_j \cdot \odot, y_j)$, with k representing the number of windings and $\odot$ the circumference of the tube. We can limit the number of windings we need to consider, since the maximum elongation distance is limited: $|k| < (2 \cdot l_p/\odot) + 1$. The $+1$ is needed because the nearest copy might be on the other side of the tube's period. Another particular of the tube as opposed to a torus is that the crossing point may lie off the tube on the finite end, so we need to check whether the y-coordinate of the crossing, $y_{crossing} = \rho_i \cdot \sin\phi_i + y_i$ is on the tube: $-0.5 \leq y_{crossing} \leq (l_{tube} - 1) \cdot \frac{1}{2}\sqrt{3} + 0.5$, where l_{tube} is the number of rings on the tube and $\frac{1}{2}\sqrt{3}$ is the height of an equilateral triangle with sides of length 1.

Supplementary Material 2: The effect of transmission speed

Transmission speed of the signal affects the spatiotemporal pattern. Our main experiment does not incorporate transmission speed; instead, it uses a fixed synaptic delay, in essence assuming transmission speed to be fast enough not to matter on that scale. This supplement explores that assumption. How fast a transmission speed is fast enough, and how slow is too slow?

To investigate this issue, we extended the model to include transmission speed. The basic model only works in terms of abstract, size-less cells, so in order to arrive at a delay value using realistic transmission speeds we added a cell size parameter in addition to the transmission speed variable. The effect of transmission speed over a connection between two cells, i and j is modelled as a delay $t_{i,j}$ which is dependent on a) the transmission speed variable, v; b) the distance between connected cells in terms of cell-breadths, $c_{i,j}$ (for distant connections this is $\rho_i + \rho_j$—see the section on distant connection implementation above—and for nearest-neighbour connections this is 1); c) the cell size variable, s. These interact in the obvious way: $t_{i,j} = \frac{c_{i,j}s}{v}$. This transmission delay was added to the base synaptic delay of 2 ms.

The cell size parameter was set at 50 μm as eukaryote cells generally range between 10 and 100 μm and there is no good reason to assume anything else.

Regarding transmission speeds, for modern-day, human neurons the values vary between .5 m/s up to roughly 100 m/s. The giant squid axon achieves 27 m/s. These higher speeds are clearly the result of secondary adaptations to improve conduction speed: myelin for the human neurons and large diameter for the squid. Slower, unmyelinated human neurons are a good baseline to investigate how slow is too slow. We performed a parameter scan over transmission speeds between .01 and 10 m/s, increasing logarithmically. We also included an infinite speed condition, reflecting the parameters used in the main experiment, for ease of comparison. The proportion of cells with elongations was fixed at 50%. We scanned all body sizes and elongation lengths 0, 2, and 4.

Figure 1 shows the results of this experiment, arranged to accentuate the effect of transmission speed. Faster but realistic transmission speeds have results similar to having an infinite transmission time. The generally observed patterns break down entirely for the slowest transmission speed (0.01 m/s). Within

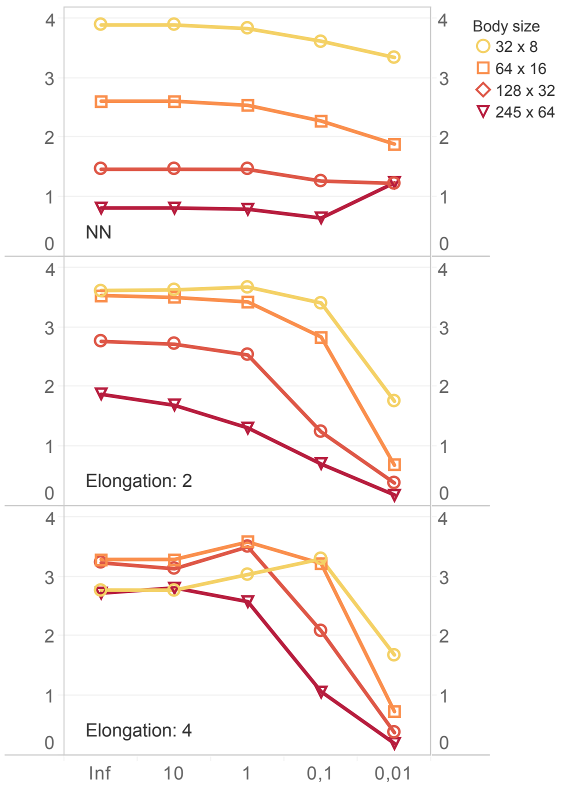

Figure 1: Illustration of how variation in transmission speed affects the patternedness measure (y-axis). Transmission speed (x-axis) decreases from left to right. Patternedness remains similar as transmission speed decreases to 1 m/s. Individual graphs represent elongation lengths: the top graph represents nearest-neighbour; the bottom graph a distance of 4 cells. Different body sizes are differentiated by color and point shape. There is no variation since these are single experiments.

any transmission speed category greater than 0.01 m/s, increasing elongation length still improves patternedness in cases where it otherwise would, indicating that given a sufficiently fast yet reasonable transmission speed the effect of elongations holds.

Supplementary Material 3: Additional notes on pattern quantification

The constant n, denoting the number of segments into which the modelled body is divided, requires more scrutiny. The analysis yields different outcomes for different values of n. This supplement aims to provide an explanation of why we chose to set the number of segments to 16 instead of iterating over it or choosing another value.

First of all, we use a power of two when setting the length of our model. We force our segments to all have the same length and thus our possible choices for the number of segments are limited to powers of two as well. The shortest length used is 32, that is 2^5 and thus we have $2, 4, 8, 16$ and 32 to pick from. The values 2 and 4 are theoretically allowable but do not fit our intuition on wave propagation. The value 32 is also allowed on theoretical grounds, but already nearest neighbor connections alone will spread out of the bin within a single time bin. This leaves us with two prima facie suitable candidates: $n = 8$ and $n = 16$, which we evaluated here.

Succinctly put, the qualitative results are similar when using different number of segments. Figure 2 shows that there is a difference in actual values but hardly a difference in overall shape. The effect of a lower number of segments is twofold: first, it causes patternedness to be higher for faster ring-shaped patterns. The optimum values will thus be biased towards longer elongation lengths, as those provide faster pattern propagation. Second, since more segments allows finer measurement the higher number of segments is able to show higher values overall. Even neat patterns within a large segment result in some lost signal. This also results in the effect visible in figure 2, where 8 segments (top graph) for small systems (yellow circles) produces an improvement in patternedness between not having elongations at all and having elongations of length 2, since the broader patterns generated by elongations allow the segments to fill out whereas smaller segments get filled out even with patterns 1 cell wide.

Since the aim of our study is to establish qualitative changes in whole-body coordination, having a measure that is constant across multiple body sizes is important, and dividing the body-tube in a fixed number of segments accom-

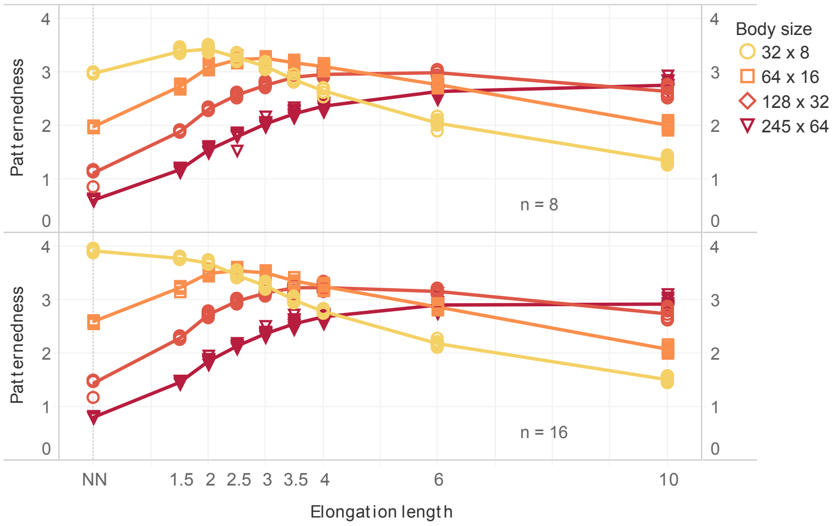

Figure 2: Illustration of variation in segment number affecting the patternedness measure. Individual graphs represent segmentation options: the top graph represents 8 segments whereas the bottom graph represents 8 segments. Different body sizes are differentiated by color and point shape. Again, patternedness is shown on the y-axis, the different elongation lengths are on the x-axis. The points scattered around the graph indicate the 10 individual model iterations which were performed for each condition and the line represents the average.

plishes this. Whether that is 8 or 16 is of secondary importance for the purposes of this study.